Journal of Nuclear Materials 402 (2010) 124–129

Contents lists available at ScienceDirect

Journal of Nuclear Materials

journal homepage: www.elsevier.com/locate/jnucmat

Analyses of crud deposits on fuel rods in PWRs using Mössbauer spectroscopy

J.A. Sawicki *

Interatomics, Victoria, British Columbia, Canada V8P 1E3

ARTICLE INFO

Article history:
Received 19 January 2010
Accepted 6 May 2010

ABSTRACT

To assess the influence of boron iron compounds deposited on fuel rods on unexpected power shifts in pressurized water reactors, samples of crud scrapes retrieved during refuelling from three reactor cores were analyzed using ^{57}Fe Mössbauer spectroscopy. The fuel crud scrapes were found to contain predominately nickel–iron ferrite $Ni_xFe_{3-x}O_4$ in a composition range $0.6 < x < 0.8$, that is with nickel content markedly higher than $0.3 < x < 0.6$ found in low boiling duty PWRs. Bonaccordite, Ni_2FeBO_5, was found only in scrapes from a core that experienced Axial Offset Anomaly of up to −12% in the beginning of examined cycle and as high as −15% in the preceding cycle. The absence of Ni_2FeBO_5 in fuel crud scrapes from two other cores is in accord with the lack of AOA during examined fuel cycles in these cores.

1. Introduction

The Axial Offset Anomaly (AOA) is a major impediment to increases in reactor fuel performance preventing PWRs from operating with even more efficient core designs than they are at present. It is a phenomenon where boron compounds such as lithium metaborate $LiBO_2$ and nickel–boroferrite Ni_2FeBO_5 (known as mineral bonaccordite) concentrate and precipitate during reactor operation in corrosion products deposited on high-duty fuel assemblies at subcooled nucleate boiling conditions and cause the unscheduled deviation in the reactor neutron flux and core axial power distribution from the predicted distribution [1–6]. Because of the very high neutron capture cross section for ^{10}B, only a small amount of precipitated boron is necessary to cause the AOA. Until now at least 40 fuel cycles in 16 PWR's in the United States and some abroad have experienced AOA. At one core, henceforth called core C, AOA eroded shutdown margins to the extent that forced the unit to operate at markedly reduced power for the final 6 months of an operating cycle. Intensive, but expensive ultrasonic fuel cleaning campaigns [6,7] as well as progress in reducing corrosion product inventory in reactor coolant by applying an elevated pH, have helped to minimize the concerns of severe AOA effects. More research is needed however to elucidate conditions at which boron-bearing solids do deposit on fuel and how to avoid their formation in high-power density reactor cores.

In our previous papers [1,3] Mössbauer spectroscopy was shown to be a suitable and versatile technique to determine the phase composition of fuel crud samples, and especially a fraction of bonaccordite in them. The purpose of the present study was to obtain the Mössbauer spectra of selected fuel crud scrapes from three reactor cores having different operational history and to determine the quantity of Ni_2FeBO_5 and other iron-bearing phases in obtained scrapes in relation to performance of these reactors.

2. Cores and samples examined

The samples removed from three different pressurized water reactor cores henceforth called C, V and S have been examined.

Core C was a high-boiling duty core that during its previous Cycle 9 has encountered the highest AOA (up to –15%) reported thus far in the PWR fleet. The axial anomaly plots in core C Cycles 9 and 10 as a function of fuel burnup are compared in Fig. 1. When the AOA in core C Cycle 9 reached −15%, the reactor was forced to operate at 30% reduced power for the final 6 months of the cycle. Characterization of fuel crud scraped after the end of this cycle has shown that Ni–Fe borate Ni_2FeBO_5 was a major component (about 50 wt.% of total Fe) in the deposits [1–3]. This highly insoluble compound can be a potent contributor to axial anomaly. Therefore, minimizing its amount in the core is a component of AOA mediation program. By design, the boiling duty in subsequent Cycle 10 was reduced significantly although the reactor encountered an immediate AOA of −12% after start of cycle, which was apparently driven by once burned assemblies carried over from Cycle 9.

Core V represented a high-temperature core operating with modified pH in the 6.9–7.4 range. AOA was not observed in the cycle under study, but it was observed in previous cycles. The scraped assembly represented medium duty compared to the previously characterized crud from the high-duty C10 rods. Core S represented a very high-boiling duty (total boiling mass), but this core has never shown any indication of AOA. Crud composition in core S may account for some differences between plants, because plant S has large-area steam generators with Alloy 690 tubes. Thus,

* Tel.: +1 250 200 6923.
E-mail address: jasawicki@shaw.ca

0022-3115/$ - see front matter © 2010 Elsevier B.V. All rights reserved.
doi:10.1016/j.jnucmat.2010.05.007

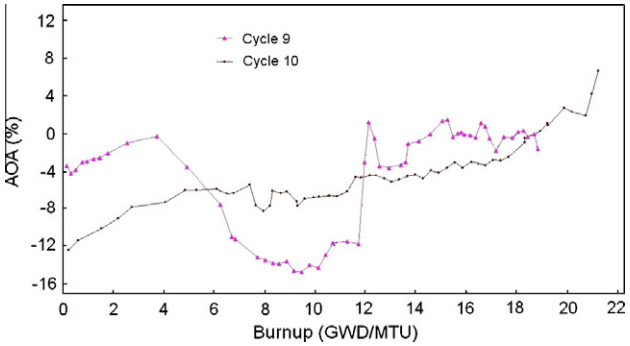

Fig. 1. Axial anomaly as a function of fuel burnup in core C during Cycles 9 and 10.

plants V and S did not experience and did not need to undertake any measures to prevent AOA in the period prior to this examination.

All crud scrapes studied here were collected by Westinghouse crews on standard-size 47-mm filter membranes and were pre-examined in the Westinghouse laboratories. The scrapers heads were made of precipitation hardening steel 17-4PH (stainless steel grade 630) that contained 15.5–17.5 wt.% chromium, 3–5 wt.% nickel, 3–5 wt.% copper and 0.3 wt.% niobium.

The most important characteristic in selecting samples for Mössbauer spectroscopy analyses was the amount of sample. In presence of the strong background radiation form the radioactive crud samples the signal to noise ratio in Mössbauer spectroscopy is low, so the analysis of samples with less than 3 mg of sample was not expected to be successful.

Light microscopy was the primary technique used to select the samples. Consideration was also given to the initial gross gamma activity and the SEM and XRD analyses performed by Westinghouse. Samples with numerous crud flakes were preferred to samples with no crud flakes. This was because boron concentration in AOA cores is thought to take place in thick crud rather than thin crud, and thick crud is more likely to fragment into discrete flakes. By selecting samples with flakes, the analysis will be more likely to reveal information on crud structure that will be relevant to AOA.

The list of samples examined by Mössbauer spectroscopy and some of the related reactor and fuel characteristics are given in Table 1 in columns 1–6. The contact doses measured for individual samples are listed in columns 7–9. The crud in all samples was largely in the form of a filter cake, while loose flakes were not present in any significant quantity. Fig. 2 shows on optical image of one of the few crud flakes observed in Cycle 10 samples. Note that in the case of the core C Cycle 9 samples such loose flakes were abundant and could be analyzed separately from the filter cake.

Out of 32 core Cycle 10 samples collected in total three were selected for Mössbauer analysis. Out of 26 samples available from V scraping campaign two have been selected that had the highest

Fig. 2. Light micrograph of a small fragment of sample C1 extracted from core C after Cycle 10.

gross gamma dose rate when the samples were retrieved. No ICP analyses were performed for the V samples so the total mass of material was not known for any of the filters. However, from the gamma activity, we inferred that the total crud mass for V samples was near 4 mg (as oxides). Finally, out of 37 samples from core S two have been chosen for Mössbauer analysis.

Small 0.5 cm^2 fragments of the filters were analyzed using gamma spectrometer equipped with a Canberra high-purity coaxial Ge detector. The gamma-emitting radioisotopes identified in the samples and their relative activities are listed in Table 2. All the data have been referenced to the date of reactor shutdown after which the crud samples was collected. The activities were measured long after the respective shutdowns; 919 days for core C, 297 days for core V and 677 days for core S samples. Therefore, only long-lived radioisotopes with high enough initial activities could be detected. At the time of analysis, the major radioisotopes in the samples were ^{60}Co and ^{54}Mn. After decay correction of the data to respective shutdown dates the dominant activity was due to ^{58}Co. The corrected to shutdown date average ^{58}Co/^{60}Co activity ratio was very high in core S (~400), smaller in core V (100), and very small in core C (45).

3. Mössbauer spectroscopy analyses

Mössbauer spectra of ^{57}Fe were obtained to determine the phase composition of iron-bearing compounds in the scraped crud samples. Mössbauer spectroscopy of such radioactive samples is rather difficult, because: (i) the β- and γ-radioactivity produces high radiation fields and background; as well as electrostatic charging of the particulates; (ii) the amount of loose scraped material on filters is miniscule, so it is impossible to prepare absorbers

Table 1
Samples and their characteristics.

Core/sample	Assembly	Face/rod/span	Assembly power	Rod power	Shutdown date	γ-contact dose (mR/h)	β/γ-contact dose (mR/h)	α-contact dose (counts/min)
C1	M46 (2 burns)	2/9/5B	1.23	1.23	02/10/99	800	400/80	5000
C2	L31 (2 burns)	2/4/6A	0.50	0.71		1300	1400/200	12,500
C3	M89 (1 burn)	1/9/6	1.27	1.31		800	200/50	3000
V1	5Y61 (1 burn)	1/9/6A	1.31		04/07/01	360	1200/200	1000
V2	5Y61 (1 burn)	1/7/6A	1.31			240	1000/150	800
S1	P55 (1 burn)	4/11/6B			06/07/00	23	0/15	250
S2	P56 (1 burn)	3/16/5B				25	0/15	350

Note: γ-contact doses were determined at plant shortly after removal of crud from the fuel. β/γ-contact doses given in column and α-contact doses were determined just after receipt of specimens in Chalk River Laboratories.

Table 2
Gamma activities of crud samples decay-corrected to reactor shutdown dates.

Isotope	^{54}Mn	^{58}Co	^{65}Zn	^{60}Co	^{95}Zr	^{95}Nb	^{113}Sn	^{125}Sb	
$T_{1/2}$	312.2 d	70.9 d	243.8 d	5.27 y	64.0 d	35.0 d	115.1 d	2.76 y	
Sample	% of total activity								Total (μCi)
C1	3.3	92.5	–	2.9	–	–	0.9	0.2	4.34
C2	4.4	90.1	–	4.4	–	–	0.6	0.3	25.6
C3	2.0	59.6	–	1.2	–	36.2	0.8	0.1	6.92
V1	10.0	52.2	21.9	0.6	4.6	9.7	0.4	0.3	6.83
V2	10.3	54.7	21.4	0.5	3.9	8.3	0.5	0.3	6.23
S1	2.8	82.2	0.9	0.2	4.6	9.0	0.2	–	6.82
S2	2.0	78.9	0.9	0.2	7.9	9.8	0.2	0.03	7.98

of suitable form and uniform optimal density; (iii) the spectra are complex and exhibit considerable line broadening due to elemental and phase composition, very small size of particles, and radiation damage processes during deposit formation; (iv) the wear of the stainless steel scraping tools itself results in collection of wear particles on the filters.

The Mössbauer absorbers were prepared using one half portion of each filter. The resonant spectra of the 14.4-keV ^{57}Fe γ-rays were recorded in transmission geometry using the 50-mCi Amersham single-line Mössbauer ^{57}Co source in a 6-μm rhodium matrix and a Reuter–Stokes Kr–CO_2 proportional counter. The velocity scale of the spectrometer was calibrated with an absorber made of 7-μm-thick natural α-Fe foil. Each spectrum was recorded for at least 20 days to acquire adequate counting statistics.

The obtained Mössbauer spectra are shown in Figs. 3–5. The spectra of all samples comprised of up to four Zeeman sextuplets of broad absorption lines and two quadrupole split doublets. The spectra were fitted to reference patterns of Ni_2FeBO_5, $NiFe_2O_4$, $Ni_xFe_{3-x}O_4$ and α-FeOOH, γ-FeOOH, and other iron-bearing compounds and alloys. The variables used in the interpretation of multiplets and in the least-squares fitting procedure were: δ_{Fe}, the centroid shift relative to that of α-Fe at 295 K; ΔE_Q, the quadrupole splitting at the iron sites; H, the hyperfine magnetic field at the iron sites; W, the half maximum line width for the Lorentzian lines; and the fractions of Fe in different spectral component (phases).

In addition to the spectral components discussed above, all the Mössbauer spectra showed a sextuplet of broad absorption lines with a relatively small separation. The fractions of iron in this form varied between 6% and 20% in various samples, and were the highest in C10 samples. This spectral component was ascribed to the particles of stainless steel 17-4PH used in the scraper heads. The parameters of the reference spectrum of such steel (cf. Fig. 1, bottom) are $H_{eff} = 26.7$ T, $\delta_{Fe} = -0.02$ mm/s, and $W = 1.38$ mm/s (W stands for line width of external lines in the sextuplet). All the Mössbauer spectra of fuel crud scrapes were analyzed assuming the presence of 17-4PH steel particles, with the initial parameters determined from the reference spectrum. Results of Mössbauer phase analysis are listed in Table 3 in percentages of total iron and corresponding weight percentages.

The least squares fits were performed using a modified Marquardt-Levenberg method. Various working assumptions were tested to obtain the most self-consistent sets of final parameters and the lowest X^2 value. The quantity X^2 is identical with the merit function Φ to be minimized by least-squares fitting routine, except for the normalization: $X^2 = \Phi/(N-M)$, where N is the total number of data points and M is the total number of free parameters. For a correct model X^2 has the statistical expectation value 1.

The final fits were performed assuming 2 or 3 sextuplets and 1 or 2 doublets (represented by 26–33 parameters), with as few as possible (between 10 and 15) constrained parameters. The individual multiplets and their envelopes are represented by full lines in Figs. 3–5. The results of the least-squares analyses showing the fractional areas under individual spectral components (as a percent of the total spectrum area) are listed in Table 3. The errors given are the 1σ statistical errors. The characteristics of the quality of fits are given in the last two columns.

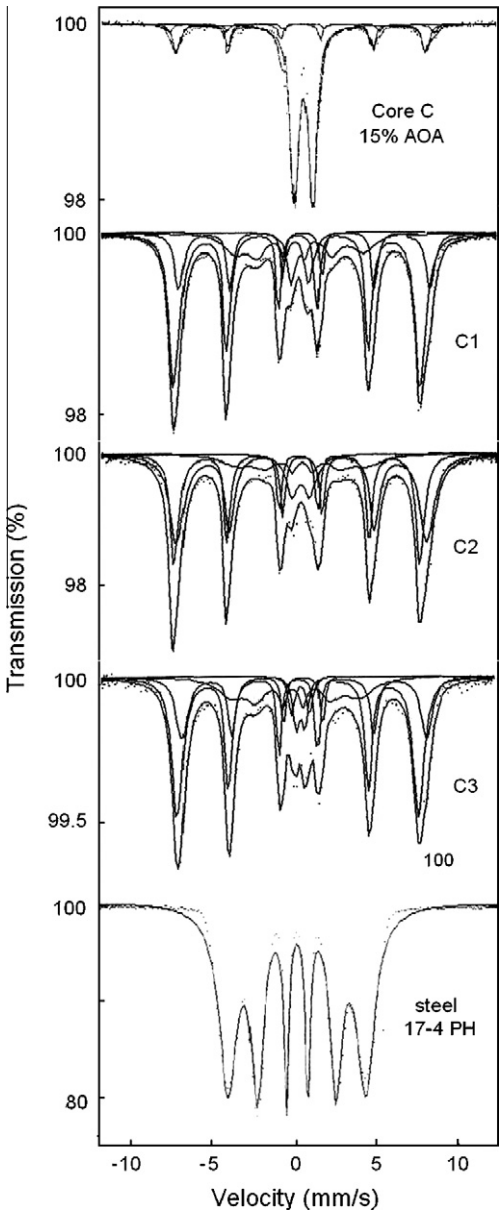

Fig. 3. ^{57}Fe Mössbauer transmission spectra obtained of core C fuel crud scrapes and reference spectrum of 17-4PH steel used in scraping tool.

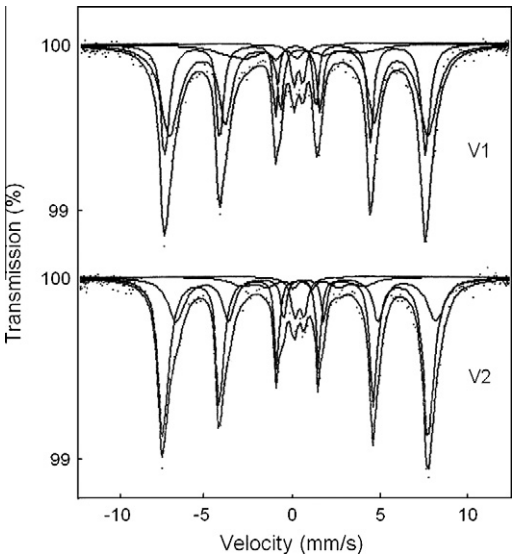

Fig. 4. ^{57}Fe Mössbauer transmission spectra of core V fuel crud scrapes.

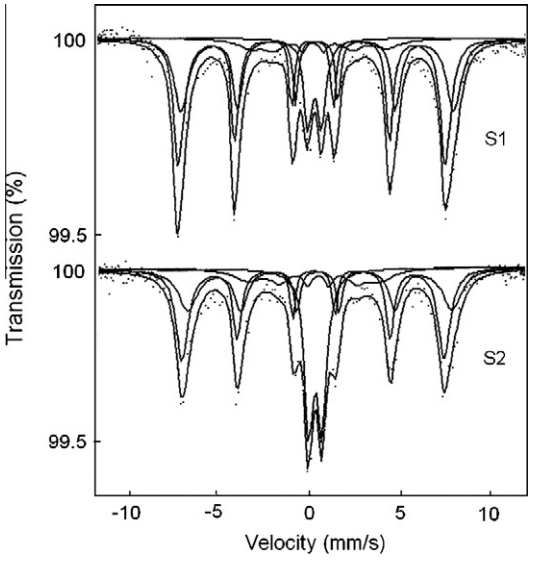

Fig. 5. ^{57}Fe Mössbauer transmission spectra of core S fuel crud scrapes.

The prominent spectral component consisting of sextuplets was ascribed to a $Ni_xFe_{3-x}O_4$ spinel ferrite, containing a considerable excess of Fe^{3+} ions, and likely some Cr^{3+} ions. The features of the $Ni_xFe_{3-x}O_4$ component were quite similar to each other in all spectra examined. The magnetic properties and conductivity mechanism of mixed-valence spinel ferrites, as well as the characteristics of their Mössbauer spectra strongly depend on the charge state and size of the substituting metal ion, and thus its affinity to occupy A- or B-sites in the spinel lattice. In the mixed-valence system $Ni_xFe_{3-x}O_4$, iron occurs in two different valency states, Fe^{2+} and Fe^{3+}, and the substitution of Fe^{2+} for Ni^{2+} takes place only in octahedral B-sites for all substitution values $0 < x < 1$, as denoted by the formula $(Fe^{3+})[Ni^{2+}{}_xFe^{2+}{}_{1-x}Fe^{3+}]O_4$ [8].

$Ni_xFe_{3-x}O_4$ is antiferromagnetic at room temperature for x from 0 to 1, while its electric conductivity decreases from almost metallic type at $x = 0$ (the band model holds up to $x = 0.6$) to n-type semiconductive at $x = 1$. Linnett and Rahman [8] reported Mössbauer study of the $Ni_xFe_{3-x}O_4$ system for $x = 0.2$, 0.4, 0.6 and 0.8. When comparing Mössbauer spectra reported by them with those obtained here, one finds the best match of spectral features for $x = 0.6$–0.8. The observation of $Ni_xFe_{3-x}O_4$ in this high range of x values can be explained by the fact that in the samples examined now the Ni/Fe ratio was close to 1. Note that in the previously studied core C scrapes the Ni/Fe ratio was on average as high 2, but in this case a considerable amount of nickel was present as NiO and Ni_2FeBO_5 particles. As a result, the compositions of the $Ni_xFe_{3-x}O_4$ found previously in the core C scrapes and in the samples examined now were quite similar.

The features of the central doublet were somewhat different in various samples. In the spectra of C samples the centroid shift and splitting of the doublet were consistent with the values known for bonaccordite, $\delta_{Fe} = 0.37$ mm/s and $\Delta E_Q = 1.17$ mm/s [3,9,10]. However, the fractional intensity of this doublet (<10%) in the C10 samples was considerably smaller than in the case of core Cycle 9 samples (cf. Fig. 1 and Table 4 in Ref. [3]); in the case of the C9 samples the central doublet dominated the spectra of crud flakes (but was considerably smaller in the spectra of the filter cake) and was, in conjunction with the results of other analytical techniques, ascribed to bonaccordite, Ni_2FeBO_5.

Ni_2FeBO_5 was found previously [1,3] in large quantities (~50% of the total iron present) in core C9 crud flakes scraped from once-burnt high-power and high-AOA fuel rods. In the present study, some – but considerably smaller – amounts of Ni_2FeBO_5 (<10% of the total iron present) could be identified with confidence only in samples from core C. Ni_2FeBO_5, which crystallizes in the form of long slender needles is insoluble in water and is only very slightly soluble in common mineral acids. Therefore, it should not be surprising that some of the particles of Ni_2FeBO_5 formed during Cycle 9 persisted on the Cycle 10 twice-burnt rods (cf. data for samples C1 and C2). Further, because early during Cycle 10 the AOA reached –12% and later fell to –6%, it is probable that some fresh bonaccordite was formed during Cycle 10 on the first load fuel rods, or relocated from once burnt rods, as exemplified by results for sample C3. In view of the lower boiling duty and smaller degree of AOA in Cycle 10 than in Cycle 9, it is not surprising that Ni_2FeBO_5 was found in the present samples in rather small quantity, compared to the high-bonaccordite scrapes retrieved from span 6 of the feed fuel rods at the end of Cycle 9 in-Plant C [1,3].

Our previous study of fuel crud scraped from core C after Cycle 9 identified ~100-μm-thick deposits that consisted of a new type of highly porous and structured Ni-, Fe-, B-, and Zr-rich material. The analyses showed that deposits contain a large amount (about 50 wt.%) of Ni–Fe oxyborate (Ni_2FeBO_5, mineral name bonaccordite), in the form of matted ~0.1-μm-thick and ~10-μm-long, needle-like particles. An especially high density of Ni_2FeBO_5 needles was found in a 30–40-μm-thick zone on the clad side of the deposits. This compound has not previously been reported as a component of PWR fuel crud. Common fuel crud components such as nickel ferrite and nickel oxide were observed only in small quantities (about 10 wt.%).

The relative intensity of the central doublet in the spectra of samples V was even smaller, representing only 4–5 wt.% of the total spectral area. Based on the measured values $\delta_{Fe} = 0.36$ mm/s and $\Delta E_Q = 0.57$ mm/s, this doublet cannot be ascribed to bonaccordite, but rather to lepidocrocite, γ-FeOOH. Lepidocrocite could be formed in the spent fuel pool from acidic Fe^{3+} solutions by an oxidative/hydrolytic process in the pH range of 5–7.5 [11], and then collected during crud scraping and filtration.

The central doublet has distinctly higher intensity in the spectra of samples S, especially in sample S2 (20% of the total spectral area), as well as a distinctly larger magnitude of splitting $\Delta E_Q \sim 0.8$ mm/s, and markedly larger line width $W \sim 0.6$ mm/s, than in the case of γ-FeOOH. These spectral features can be best ascribed to iron oxy-hydroxide named ferrihydrite, having the approximate chemical formula $Fe_5HO_8{\cdot}4H_2O$ [11]. The Mössbauer

spectrum of ferrihydrite is best described as a distribution of overlapping quadrupole doublets having isomer shift $\delta_{Fe} = 0.35$ mm/s and two quadrupole splitting maxima at $\Delta E_Q = 0.62$ mm/s and 0.78 mm/s. Approximating such distribution of doublets by one quadrupole doublet one arrives at $\Delta E_Q \sim 0.7$–0.8 mm/s and $W \sim 0.6$ mm/s, as determined in samples S1 and S2. Ferrihydrite is X-ray amorphous and is often the initial precipitate that results from the rapid hydrolysis of Fe(III) solutions. It is not excluded that this substance was collected from spent fuel pool water during the fuel crud sampling. Ferrihydrite could have formed in acidic spent fuel pool water, for example, by briefly heating the solution (at 80 °C) or by rapidly raising the pH to ca. 7 with alkali [11].

It should be noted that, in the case of samples V and S, the presence of small fraction of Ni_2FeBO_5 could not be excluded with a great deal of certainty. This is caused by the fact that the central (near-zero velocity) part in the Mössbauer spectra of samples from both plants indicates a broad absorption signal that partly overlaps with located there absorption lines of $Ni_xFe_{3-x}O_4$, and thus cannot be unambiguously deconvoluted. As discussed above, this central part of spectrum was best ascribed to quadrupole doublet of γ-FeOOH in core V samples and ferrihydrite in core S samples. However, within the limits of the statistical accuracy and resolution of the spectra some part of these central doublets can be also attributed to Ni_2FeBO_5. Based on additional fits and simulations including possible Ni_2FeBO_5 component it was concluded that the upper limit for fractions of Ni_2FeBO_5 could be 2% Fe in core V samples and 5–6% Fe in core S samples.

Furthermore, the possibility of presence of some small quantity of $NiFeBO_4$, especially in samples from core S, cannot be as well completely excluded on the basis of Mössbauer spectra alone. According to Abe et al. [9,10], the Mössbauer spectrum of this compound at room temperature yields a quadrupole doublet described by $\delta_{Fe} = 0.44$ mm/s and $\Delta E_Q = 0.71$ mm/s; the values of these parameters are fairly close to that of ferrihydrite. Therefore, it is reasonable to assume that the fraction of iron in form of $NiFeBO_4$ in examined samples from core S cannot be larger, and most likely is smaller, than the fraction of iron in form of ferrihydrite in these samples (cf. a note under the Table 3).

In addition to the spectral components discussed above, all the Mössbauer spectra showed components consisting of six broad absorption lines with a relatively small separation. The fractions of iron in this form varied between 3% and 13% in various samples, and were the highest in C samples. The effective magnetic hyperfine field associated with this component had a value in the range $H_{eff} \sim 25$ T that is almost two times lower than in the case of $Ni_xFe_{3-x}O_4$. Based on the value of this field, very large line width, $W \sim 1.5$–2.5 mm/s (W stands for line width of external lines in the sextuplet), and the small average values of the centroid shift and quadrupole splitting obtained for this component, δ_{Fe} and $\Delta E_Q \sim 0$ mm/s, it was suggested that this form of iron represents fine particles of some ferromagnetic iron alloy. The reference Mössbauer spectrum of the steel used in the scraper heads is presented in Fig. 3 (bottom). All the Mössbauer spectra of fuel crud scrapes were re-analyzed assuming the presence of 17-4PH steel particles, with the initial parameters determined from the reference spectrum shown i.e. $H_{eff} = 26.7$ T, $\delta_{Fe} = -0.02$ mm/s, and $W = 1.38$ mm/s. The results of Mössbauer phase analysis are listed in Table 3 in percentages of total iron and corresponding weight percentages calculated as described below.

To determine the weight fractions of the identified iron compounds from their relative spectral areas more accurately one must know the Lamb–Mössbauer factors, f_a, for Ni_2FeBO_5, $Ni_xFe_{3-x}O_4$, γ-FeOOH, and 17-4PH steel. Because the value of f_a for Ni_2FeBO_5 is yet not known, it was assumed that the f_a factors for all three compounds, as well as for steel, are equal one to each other. The exact fraction of Fe in $Ni_xFe_{3-x}O_4$ is not known, but on the average the value of x can be assumed to be close to 0.7. Based on these assumptions, the molecular weight fractions given in Table 3 were derived from percentages of Fe by using the corresponding weight conversion factors: $2.3Fe/Ni_{0.7}Fe_{2.3}O_4 = 0.6$; $Fe/Ni_2FeBO_5 = 0.2$; Fe/FeOOH = 0.6; and Fe/17-4PH steel = 0.75. Because the weight fraction of Fe in Ni_2FeBO_5 is small, the conversion resulted in significant increase in weight fractions of Ni_2FeBO_5 as compared to weight fractions of other phases.

4. Discussion

In general, the fuel crud samples studied here contained predominately a mixed Ni–Fe ferrite, $Ni_xFe_{3-x}O_4$, in a composition range $0.6 < x < 0.8$ (or $0.25 < Ni/Fe < 0.4$), as expected for relatively low boiling duty PWR cores. This is a considerably higher range of x values than the range $0.3 < x < 0.6$ (or $0.1 < Ni/Fe < 0.25$) considered as typical for $Ni_xFe_{3-x}O_4$ in low and high duty PWRs in EPRI Guidelines [12]. On the other hand, the examination of data on Ni/Fe frequency distribution for 238 crud samples from low and moderate to high power fuel rods examined by Westinghouse until 1998 [13] shows a skewed, broad Gaussian-like distribution in Ni/Fe frequency that is centred around 0.5 ($x \sim 1$) and whose half-width spans the range $0.3 < Ni/Fe < 0.7$. Note that because $Ni_xFe_{3-x}O_4$ has an inverse spinel structure, the value of x cannot be higher than 1, that is, Ni/Fe ratio cannot be larger than 0.5. Thus, any measured values of Ni/Fe higher than 0.5 suggests that the crud contains not only $Ni_xFe_{3-x}O_4$ but also that it must contain nickel in some other chemical phase, such as NiO, and in extreme cases, Ni_2FeBO_5 as well.

According to existing models, the deposits of $Ni_xFe_{3-x}O_4$ are thought to form on fuel rods largely because at the operating pH range of PWR cores the solubility of iron, and to lesser degree, the solubility of nickel, decreases when the temperature increases. The computer models to optimize primary side chemistry for maximizing dissolution and minimizing deposition of Fe and Ni, such as the Siemens code [14], assume $Ni_xFe_{3-x}O_4$ with a slightly wider composition range of $0.4 < x < 0.8$. It must be emphasized that the

Table 3
Results of ^{57}Fe Mössbauer spectroscopy analyses of fuel crud samples.

Sample	Counts × 10^6/channel	$NiFe_2O_4$ %Fe	$NiFe_2O_4$ (wt.%)	Ni_2FeBO_5 %Fe	Ni_2FeBO_5 (wt. %)Fe	γ-FeOOH %Fe	γ-FeOOH (wt.%)	17-4PH %Fe	17-4PH (wt.%)	P/C	X^2
C1	30.1	78.7 ± 3.0	68.9 ± 2.6	8.4 ± 0.4	22.1 ± 1.0	–	–	12.9 ± 0.6	9.0 ± 0.4	26/12	9.5
Repeat	56.8	76.4 ± 3.6	64.4 ± 2.5	10.6 ± 0.5	26.8 ± 1.3	–	–	13.0 ± 0.7	8.8 ± 0.4	26/12	9.1
C2	7.3	83.9 ± 4.2	71.7 ± 3.6	9.2 ± 0.6	23.6 ± 1.5	–	–	6.9 ± 0.8	4.7 ± 0.6	26/12	8.4
C3	47.9	76.9 ± 4.0	68.8 ± 3.6	7.1 ± 0.6	19.0 ± 1.6	4.9 ± 0.5	4.3 ± 0.4	11.1 ± 0.8	7.9 ± 0.6	33/15	2.4
V1	17.6	92.1 ± 4.1	92.7 ± 4.1	–	–	4.5 ± 0.3	4.5 ± 0.3	3.4 ± 1.1	2.8 ± 0.9	26/13	2.6
V2	19.0	91.7 ± 4.1	92.4 ± 4.2	–	–	4.8 ± 0.4	4.8 ± 0.4	3.5 ± 1.1	2.8 ± 0.9	26/13	2.5
S1	60.5	81.6 ± 5.7	82.7 ± 5.7	–	–	13.3 ± 0.7[a]	13.3 ± 0.7[a]	5.1 ± 1.1	4.0 ± 0.9	26/10	2.7
S2	27.3	69.4 ± 4.5	68.9 ± 1.9	–	–	24.8 ± 0.8[a]	24.5 ± 0.7[a]	5.8 ± 1.2	4.6 ± 0.9	26/10	1.6

[a] Due to large line widths of the central doublet in S1 and S2 samples it is also possible to interpret this fraction as ferrihydrite or/and ferrite $NiFeBO_4$.

current models that describe the formation of $Ni_xFe_{3-x}O_4$ in mid-duty PWR cores do not yet account for the occurrence of Ni_2FeBO_5 in high-boiling duty cores.

A model that would allow us to predict the formation of Ni_2FeBO_5 in complex nuclear, chemical and hydrothermal conditions at the boiling coolant – fuel boundary in the high-duty high AOA PWR core was proposed by the author in Ref. [2]. The production of lithium in ^{10}B-n reactions and role of lithium in promotion of hydrothermal synthesis of bonaccordite are two of the most essential premises of this model. To verify the predictions of our model and in order to determine how to avoid formation and deposition of bonaccordite on fuel rods in a pressurized water reactor core we are currently studying the production rates of bonaccordite in water solutions containing iron, nickel, boron and lithium compounds at pressures typical for PWR's and as a function of temperature [15].

Iron phases such as lepidocrocite γ-FeOOH observed in-plant V core samples and possibly ferrihydrite in-plant S samples could be the result of hydrolysis of dissolved iron in the spent fuel pool water. On precipitation, these compounds tend to form very small and often amorphous particulates. For obtaining the more representative samples of fuel crud, in future fuel scraping campaigns the use of spent fuel pool water during scraping operation should be avoided or minimized.

5. Conclusions

In the present work we have analyzed the fuel crud scrapes from three different reactor cores using Mössbauer spectroscopy technique. The analyses showed much smaller amount of bonaccordite Ni_2FeBO_5 in the samples from all three cores than previously observed in cruds retrieved from core C that have experienced exceptionally high Axial Offset Anomaly during its Cycle 9. Small fractions of bonaccordite observed in crud from this plant after Cycle 10 suggest that the measures undertaken in the industry to minimize deposition and retention of boron and Ni_2FeBO_5 on fuel cladding surfaces are successful. The principal iron-bearing compound observed in all samples investigated here has been the nickel ferrite $Ni_xFe_{3-x}O_4$ and we have obtained some detailed information about its properties. Thus, together with the results recently obtained using other techniques, we are arriving at better and better understanding of fuel crud deposition and its properties in PWRs.

The successful application of Mössbauer spectroscopy to the analysis of fuel crud scrapes with high very specific activity allows us to predict that this technique will become more often used as an analytical tool in the nuclear power industry, not only in more routine corrosion product transport studies, but also – in particular – for rapid in-plant diagnostics of bonaccordite in fuel crud scrapes. Application of this technique directly in the radiochemical laboratory of the nuclear power plant would eliminate costly transportation of radioactive samples from the plant to a specialized research laboratory outside. Setting up the Mössbauer spectroscopy facility in the nuclear power plant and obtaining the licence for using ^{57}Co source should not be difficult. After all, it has already been proved that Mössbauer spectrometers are transportable, versatile and can operate satisfactorily even on Mars.

Acknowledgements

This investigation was funded by Electric Power Research Institute' Robust Fuel Program. The samples have been analyzed at Atomic Energy of Canada Limited Chalk River Laboratories. The author thanks J. Deshon (EPRI) and W.A. Byers (Westinghouse) for interest in this work, great help in selecting the samples and discussions.

References

[1] P.L. Frattini, J. Blok, S. Chauffriat, J.A. Sawicki, J. Riddle, Nucl. Energy 40 (2001) 123–135.
[2] J.A. Sawicki, Nuclear chemistry model of borated fuel crud, in: Proc. Int. Conf. on Water Chemistry in Nucl. Reactor Systems, April 22–26, 2002, Avignon, France.
[3] J.A. Sawicki, J. Nucl. Mater. 374 (2008) 248–269.
[4] W.A. Byers, J. Deshon, Structure and chemistry of PWR crud, in: Proc. Inter. Conf. on Water Chem. in Nucl. Reactors Systems, October 11–14, 2004, San Francisco, USA.
[5] W.A. Byers, J. Deshon, G.P. Gary, J.F. Small, J.B. Mcinvale, Crud metamorphosis at the Callaway plant, in: Proc. Inter. Conf. on Water Chem. in Nucl. Reactors Systems, October 23–26, 2006, Jeju, Korea.
[6] P.L. Frattini, T. Moser, Nucl. Energy International, August 2000.
[7] J. Blok, J. Deshon, K. Edsinger, P. Frattini, Ultrasonic fuel cleaning in PWRs and BWRs, in: Proc. Inter. Conf. on Water Chem. in Nucl. Reactors Systems, October 11–14, 2004, San Francisco, USA.
[8] J.W. Linnett, M.M. Rahman, J. Phys. Chem. Solids 33 (1972) 1465.
[9] M. Abe, K. Kaneta, M. Gomi, S. Nomura, J. Phys. Colloque C2 40 (1979) 325.
[10] M. Abe, K. Kaneta, M. Gomi, S. Nomura, Mater. Res. Bull. 14 (1979) 519–526.
[11] U. Schwertmann, R.M. Cornell, Iron Oxides in the Laboratory: Preparation and Characterization, VCH, Weinhem, New York, Basel, Cambridge, 1991.
[12] PWR Primary Water Chemistry Guidelines, vol. 2, Revision 5, TR-105714-V2R5.
[13] W.A. Byers, J.M. Partezana, The structure and chemistry of deposits on high power PWR fuel assemblies, in: Proc. 1998 EPRI PWR-BWR Plant Chemistry Conference, Huntington Beach, 1998 September, Paper 9, EPRI GC-112049.
[14] F. Becker, B. Stellwag, S. Odar, G. Probst, Using Siemens modelling to predict RCS deposition trends, in: Proc. EPRI PWR-BWR Chemistry Conference, Huntington Beach, 1988 September. EPRI GC-112049.
[15] J.A. Sawicki, Hydrothermal synthesis at PWR pressure and temperatures (in press).